

# THE FORMATION OF PLANETS AROUND STARS OF VARIOUS MASSES AND THE ORIGIN AND THE EVOLUTION OF CIRCUMSTELLAR DUST CLOUDS

Takenori Nakano  
Department of Physics, Kyoto University  
Sakyo-ku, Kyoto 606, Japan

**ABSTRACT.** The formation of planets is investigated both in a gaseous nebula and after the nebula has been blown away. The capture of planetesimals by a protoplanet is investigated by taking into account the growth of planetesimals. The time of planet formation is determined as a function of distance from the central star. The formation time of Neptune is found to be  $3.9 \times 10^9$  yr, a value shorter than the age of the solar system. The region where planets form within the stellar lifetime is determined, and it is found that only stars of mass less than several solar masses can have planets. The dust clouds around  $\alpha$  Lyrae and  $\beta$  Pictoris are far outside the planet-forming regions. A model for the circumstellar dust cloud is proposed which can explain the basic properties of the  $\beta$  Pic disk.

## 1. INTRODUCTION

Formation processes of planets around the Sun have been investigated by many authors both in a gaseous nebula (Cameron and Pine 1973; Hayashi et al. 1977, 1985) and in the gas-free state (Safronov 1969; Matsui and Mizutani 1977, 1978; Hartmann 1978; Greenberg et al. 1978, 1984; Cox and Lewis 1980). Many astronomers believe that some fraction of solar-type stars is accompanied by planets. Such interest has been enhanced by the discoveries of dust clouds around  $\alpha$  Lyrae (Aumann et al. 1984) and  $\beta$  Pictoris (Smith and Terrile 1984). However, few works have been done on the formation of extrasolar planets.

The composition and even the existence of solid materials in the gaseous nebula are determined by the temperature. The stellar luminosity influencing the temperature is very sensitive to the stellar mass  $M_*$ . The stellar lifetime is also sensitive to  $M_*$ . Therefore, the region where planets form within the stellar lifetime is rather sensitive to  $M_*$ . In Sections 2 and 3 we shall investigate the planet formation around stars of various masses and we shall determine the regions where planets may form within the stellar lifetime and the mass range of the star which may possess planets. In Section 4 we

shall investigate the origin and evolution of the circumstellar dust cloud and we shall compare the results with the observations.

## 2. PROCESSES OF PLANET FORMATION

With the limited space available for this article we are obliged to describe only the scenario of planet formation. The details will be published elsewhere.

### 2.1. Structure of the Gaseous Nebula

By analogy with the solar nebula (Hayashi 1981), we assume that the distribution of the surface density (mass per unit area)  $\sigma$  of the gaseous disk is given in units of  $\text{g cm}^{-2}$  as

$$\sigma(r) = 1.7 \times 10^3 f_{\sigma} (M_{*}/M_{\odot})^{5/6} r_{\text{AU}}^{-3/2}, \quad (1)$$

where  $r_{\text{AU}}$  is the distance from the central star in AU, and  $f_{\sigma}$  is an arbitrary parameter. The power 5/6 for  $M_{*}$  is obtained if one assumes a sort of homology. The ambiguity in the  $M_{*}$ -dependence may be dissolved by investigating over the allowable range of  $f_{\sigma}$ . When

$$f_{\sigma} > 33.2 (M_{*}/M_{\odot})^{-1/3} (T/100\text{K})^{1/2}, \quad (2)$$

$T$  being the temperature of the nebula, the gaseous disk is gravitationally unstable (Toomre 1964; Goldreich and Lynden-Bell 1965a,b), and gaseous objects much heavier than Jupiter would form. We restrict ourselves to the cases where solid planets may form. Of course the formation of Jovian planets by capturing gas thereafter is not excluded. Then, it would be sufficient to consider the cases of  $f_{\sigma} \lesssim 10$ .

Due to the gas pressure, the angular velocity  $\Omega_g$  of the circular motion of the gaseous nebula deviates slightly from the Keplerian velocity  $\Omega_K = (GM_{*}/r^3)^{1/2}$ ,  $G$  being the gravitational constant, as

$$\Omega_g^2 = \Omega_K^2 (1 - 2\eta), \quad (3)$$

where

$$\eta = - (P/2\rho v_K^2) \frac{d \log P}{d \log r}, \quad (4)$$

$\rho$  and  $P$  being the mean density and pressure, respectively, in the nebula, and  $v_K = (GM_{*}/r)^{1/2}$  being the circular Keplerian speed. This small deviation plays an important role in the migration of planetesimals as shown in Section 2.4.

### 2.2. Formation and Fragmentation of a Dust Layer

The dust grains sink gradually to the central plane of the nebula with a time scale of about  $10^3$  times the Keplerian period

$t_K = 2\pi (r^3/GM_*)^{1/2}$  (Safronov 1969; Weidenschilling 1980; Nakagawa et al. 1981). By sedimentation of dust there appears around the central plane a thin dense layer mainly composed of dust. This layer fragments into planetesimals due to the gravitational instability when the density reaches 0.17 times the Roche's density (Sekiya 1983). The mean mass of planetesimals thus formed is given by

$$m_0 = 4\pi r_s^6 \sigma_s^3 / (1.057M_*)^2, \tag{5}$$

where  $\sigma = \zeta\sigma_s$  is the surface density of solid material,  $\zeta$  being the solid mass fraction in the initial gaseous nebula. We take  $\zeta = 0.0042$  when the solid part is composed of rocky materials and  $\zeta = 0.018$  when it is composed of icy and rocky materials.

### 2.3. Kinetic States and Growth of Planetesimals

The mass spectrum of planetesimals changes with time due to collisional growth. However, except for the concluding stage of planet formation, the dominant portion of the population has a considerably smaller size than the largest bodies (Greenberg et al. 1978, 1984; Nakagawa et al. 1983). Therefore, we shall describe the planetesimals with their representative mass  $m$  without going into details of the spectrum.

The orbit of the planetesimal deviates from a circle and declines from the central plane to some extent. The mean amounts of these deviations (random motion) can be estimated in the following way.

The random motion of planetesimals is enhanced by mutual gravitational scattering with the time scale (Chandrasekhar 1942)

$$t_E = v^3 / (6.49 \pi G^2 m^2 n \ln \Lambda), \tag{6}$$

where  $v$  and  $n$  are, respectively, the random velocity and number density of planetesimals, and  $\ln \Lambda$  is a factor coming from the integration with the impact parameter and takes a value of about 10.

The direct collision of planetesimals is highly dissipative (Fujiwara and Tsukamoto 1980). The random motion decays by the direct collision with the time scale

$$t_C = (4\pi a^2 n v)^{-1} (1+2\theta)^{-1}, \tag{7}$$

where  $\theta$  is the so-called Safronov number given by

$$\theta = Gm / (av^2). \tag{8}$$

and  $a = (3m/4\pi\rho_s)^{1/3}$  is the radius of the mean planetesimal,  $\rho_s$  being the density of solid matter. We take  $\rho_s = 3 \text{ g cm}^{-3}$  when it is composed of rocky materials and  $\rho_s = 1 \text{ g cm}^{-3}$  for icy and rocky materials.

The gas moves circularly nearly with the Keplerian speed. Therefore, the random motion of planetesimals is also dissipated by the gas drag force which may be written as

$$\mathbf{f} = -\frac{1}{2} C_D \pi a^2 \rho \mathbf{v} \cdot \mathbf{v}. \quad (9)$$

Because the gravity of the planetesimal exerts some influence upon the fluid motion around it, the coefficient  $C_D$  may be written for the subsonic flow as

$$C_D = C_1 + C_2 (Gm/ac_s^2)^2, \quad (10)$$

where  $c_s$  is the sound speed in the gas. We find that the results of numerical simulations on the fluid motion around a solid body by Takeda et al. (1985) can be well represented by equation (10) with  $C_1 = 2.5$  and  $C_2 = 0.7$ . The dissipation time of the random motion by the gas drag force is given by

$$t_g = 2m / (\pi C_D a^2 \rho v). \quad (11)$$

The mean eccentricity  $e$  and inclination  $i$  of the orbits of planetesimals are related to the random velocity  $v$  and the Keplerian speed  $v_K$  as

$$e \approx i \approx v/v_K. \quad (12)$$

The number density of planetesimals is given by

$$n = \sigma_s / (2\pi r i). \quad (13)$$

The random velocity changes with time according to

$$v^{-2} \frac{d}{dt} v^2 = t_E^{-1} - t_c^{-1} - t_g^{-1}. \quad (14)$$

Because the direct collision is mostly coalescent as confirmed below, the representative mass of planetesimals grows with time according to

$$\frac{1}{m} \frac{dm}{dt} = 1/t_c. \quad (15)$$

In the gaseous nebula with  $f_{\sigma} \gtrsim 1$  we find  $t_c > t_g$ , and then the relaxation of the random velocity is faster than the collisional growth. Therefore, the steady state is approximately given by

$$t_E^{-1} = t_c^{-1} + t_g^{-1}. \quad (16)$$

In the gas-free state with  $t_g = \infty$ , we find with the help of equations (6) to (8) that the steady state for equations (14) and (15) is given by

$$0.6/t_E = 1/t_c. \quad (17)$$

For the random velocity determined by equation (16) or (17) we find  $\theta \gtrsim 0.4$  irrespective of the representative mass  $m$ . This means that the gravity of planetesimals is important in their collision.

Because the collision is highly inelastic, the energy of relative motion is efficiently dissipated, and then they mostly coalesce by their gravity.

The growth of planetesimals is obtained by integrating equation (15) with the random velocity determined by equation (16) or (17) and with the initial mass  $m_0$  given by equation (5). The representative mass  $m$  soon becomes insensitive to  $m_0$ .

#### 2.4. Growth of the Protoplanet

So far we have investigated the growth of the representative mass of planetesimals. However, the mass of planetesimals spreads to a considerable extent by random coalescence. We call the most massive object in some specified region a protoplanet. While planetesimals grow by mutual sticking, they are gradually captured by the protoplanet.

Let us consider a protoplanet of mass  $m \geq 10^2 m_p$ . Because the excitation time of its random velocity by collisions with planetesimals is greater than the age of the protoplanetary system, its random velocity is not greater than the random velocity of the mean planetesimal (Nakano 1986). Therefore, the collision cross section of the protoplanet with a planetesimal is much greater than the geometrical cross section, and then the protoplanet captures the planetesimals whose orbital semimajor axis is close to its own in a time scale considerably smaller than the age of the system (Nakano 1986).

However, the protoplanet can hardly capture the planetesimals with considerably different orbital semimajor axis. Such planetesimals are captured only after their semimajor axis has approached that of the protoplanet. The orbit of a planetesimal varies by mutual gravitational scattering and by the gas drag force. The orbital semimajor axis of the mean planetesimal changes by the mutual scattering by a factor of 2.72 (the base of natural logarithm) in a diffusion time (Hayashi et al. 1977)

$$t_d = t_E (v_K/v)^2. \quad (18)$$

The gas motion is nearly completely circular, parallel to the central plane, and slightly deviates from the Keplerian speed as shown by equation (3). Therefore, the circular motion as well as the random motion of planetesimals are dissipated by the gas drag force. Assuming that the variation of the orbit of a planetesimal in a Keplerian period is small and  $\eta \ll e \approx i \ll 1$ , we have investigated the work of the gas drag force on a planetesimal, and found that the total energy  $E$ , and then the semimajor axis, of the planetesimal decrease by a factor 2.72 in a flow time

$$t_E = |E/\dot{E}| \approx t_g / (2\eta + \frac{5}{8} e^2 + i^2), \quad (19)$$

where  $t_g$  is the time scale given by equation (11) averaged over the Keplerian period. Equation (19) agrees well with the flow time given by Hayashi et al. (1977).

Let  $\Delta r = c_m r$  be the mean migration distance of planetesimals, i.e., the mean variation of the orbital semimajor axis suffered by the planetesimal before it is captured by the protoplanet. Then the migration rate of the planetesimal is given by

$$(c_m^2 t_d)^{-1} + (c_m t_f)^{-1}. \quad (20)$$

As long as a protoplanet much more massive than the mean planetesimal exists, equation (20) gives the capture rate of the planetesimal. Because  $\Delta r \approx (r_{n+1} - r_n)/2$ , a half of the orbital distance of the resultant adjacent planets, we take

$$c_m = \frac{1}{2} \ln (r_{n+1}/r_n). \quad (21)$$

In the solar system  $r_{n+1}/r_n$  lies between 1.3 and 2.0. We shall use  $c_m = 0.20$  corresponding to the mean value  $\langle r_{n+1}/r_n \rangle \approx 1.5$ .

Both  $t_d$  and  $t_f$  are functions of the position  $r$  and the mean mass  $m$  of planetesimals, and  $m$  is a function of time  $t$  through equation (15). Therefore, the migration rate given by equation (20) is a function of  $r$  and  $t$ . We can consider that the planet forms when most of the planetesimals in a specified region have been captured by the protoplanet, i.e., at a time  $t$  satisfying

$$t^{-1} \approx (c_m^2 t_d)^{-1} + (c_m t_f)^{-1}. \quad (22)$$

In the gas-free state we take  $t_f = \infty$ . Equation (22) determines the time of planet formation  $t_{pf}$  as a function of  $r$ .

It is to be noticed that equation (22) determines  $t_{pf}$  only when an object much more massive than the mean planetesimal already exists. As seen in the numerical simulations (e.g., Greenberg et al. 1978, 1984), some objects of mass greater than  $10^2 m_0$  already exist when the representative mass becomes about  $10 m_0$ . Therefore, we consider that the planet forms at the time  $t$  when both of the following two conditions are satisfied for the first time: (i) the migration rate given by equation (20) exceeds  $t^{-1}$ , and (ii) the mean mass  $m$  is greater than  $10 m_0$ . In most cases condition (i) actually determines the epoch of planet formation.

### 3. NUMERICAL RESULTS ON PLANET FORMATION

According to the theory on the structure of Jupiter (Hubbard et al. 1980), its core mass amounts to 20 to 30 times the Earth mass  $M_E$ . Therefore,  $f_\sigma \approx 2$  seems more suitable to the solar system than  $f_\sigma = 1$ . Figure 1a shows the time of planet formation  $t_{pf}$  as a function of  $r$  for  $M_* = 1 M_\odot$ ,  $f_\sigma = 2$ , and  $c_m = 0.20$ . The dashed line represents  $t_{pf}$  in the gaseous nebula and solid line in the gas-free state. The step on the dashed line corresponds to the state of  $T = 170\text{K}$ . We have assumed that the planetesimals are composed of rocky materials in the inner region, and icy and rocky materials in the outer region. For the gas-free state we have assumed that such transition occurs at

$T = 100\text{K}$  due to the lower sublimation temperature at lower pressure (Gaustad 1963). Because the gaseous nebula must have been blown away in the early stage of the solar evolution, probably at  $t \approx$  several  $\times 10^7$  yr (Sekiya et al. 1980), the planets in the inner region must have formed in the gaseous nebula and those in the outer region in the gas-free state. The Earth formed at  $t \approx 1.7 \times 10^6$  yr in the gaseous nebula, and Neptune at  $t \approx 3.9 \times 10^7$  yr, within the age of the solar system, even in the gas-free state. This is in remarkable contrast with the previous theory which derived  $1 \times 10^{11}$  yr as the formation time of Neptune (Safronov 1969). Within the lifetime of the Sun  $1 \times 10^{10}$  yr planets form only at  $r \lesssim 46\text{AU}$ .

Figure 1b shows the time of planet formation  $t_{pf}$  for  $M_* = 2M_\odot$ ,  $f_\sigma = 2$ , and  $c = 0.20$ . Planets form only at  $r \lesssim 10\text{AU}$  within the stellar lifetime  $1.3 \times 10^9$  yr.

We have also investigated the formation of planets around stars of  $M_*/M_\odot = 0.5, 0.7, 3, 5,$  and  $10$ . Figure 2 has been compiled from all the results. The solid line shows the position where  $t_{pf}$  is equal to the stellar lifetime for  $f_\sigma = 2$ . The dashed lines  $t_{pf}$  show the positions of constant temperature. The fraction of matter which is in the solid state becomes very small at  $T \geq 1300\text{K}$  (Grossman 1972). Therefore, planets can form only in the region surrounded by the solid line and the dashed line with  $T = 1300\text{K}$ . Therefore, only stars of mass less than several solar masses can have planets. The dot-dashed line shows the position where  $t_{pf}$  is equal to the stellar lifetime for  $f_\sigma = 10$ . The planet-forming region in this case is slightly larger

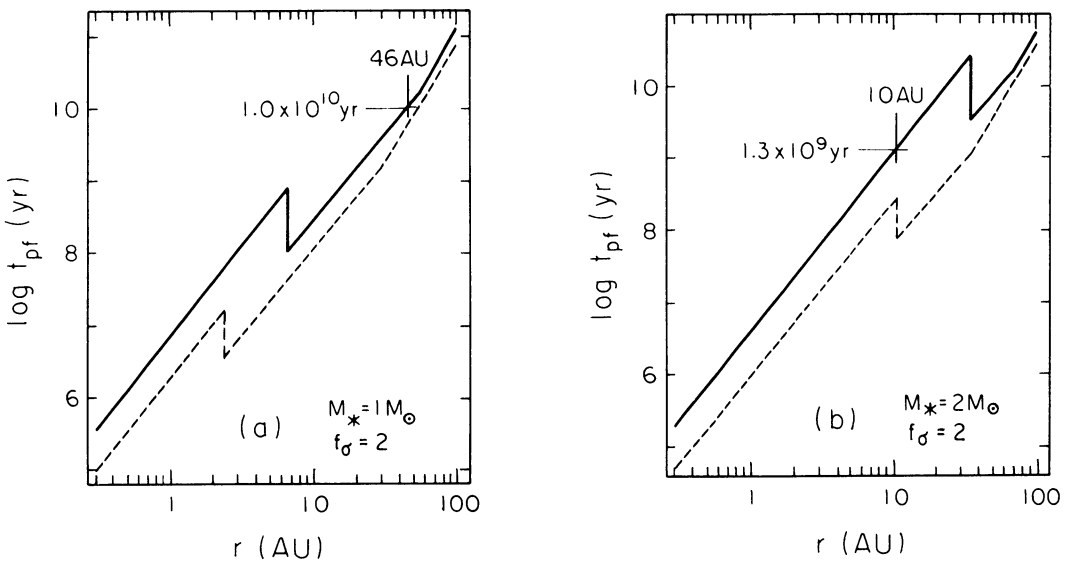


Fig.1. The planet formation time  $t_{pf}$  as a function of the distance  $r$  from the central star of  $M_* = 1M_\odot$  (a) and  $2M_\odot$  (b) for  $f_\sigma = 2$  and  $c = 0.20$ . The dashed line represents  $t_{pf}$  in the gaseous nebula and the solid line in the gas-free state.

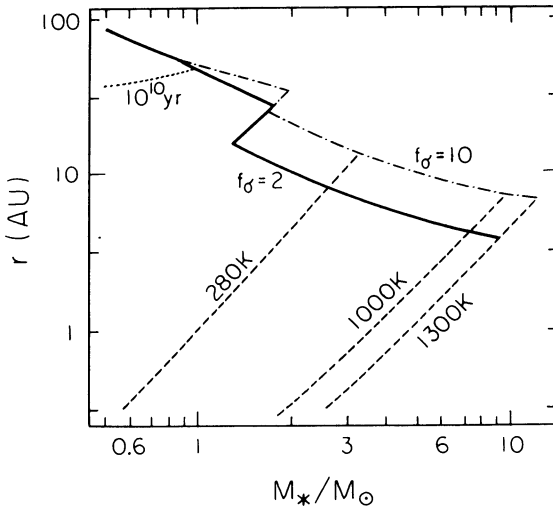


Fig.2. The planet-forming region as a function of the stellar mass  $M_*$ . Planets form within the stellar lifetime inside the solid line for  $f_\sigma = 2$  and inside the dot-dashed line for  $f_\sigma = 10$ . Planets hardly form in the region with  $T \geq 1300\text{K}$ .

than in the case of  $f_\sigma = 2$ . Only stars of  $M_* \lesssim 3M_\odot$  can have a planet on which the temperature is nearly equal to that of the Earth (280K) and living things can exist at least with respect to the temperature.

#### 4. A MODEL FOR CIRCUMSTELLAR DUST CLOUDS

Alpha Lyrae has a dust cloud emitting thermal radiation of about 85K from a region of radius around 85AU (Aumann et al. 1984). From its luminosity  $L_* = 58L_\odot$  the mass of  $\alpha$  Lyr is estimated to be between  $2.5$  and  $2.9M_\odot$ . Smith and Terrile (1984) found that  $\beta$  Pictoris is accompanied by a dust disk nearly edge-on to us whose radius is at least 400AU. The mean inclination of the orbits of dust in this disk is less than  $5^\circ$  at  $r \approx 300\text{AU}$ , and the distribution of the surface brightness on the central plane is approximated by the power law  $r^{-4.3}$  at the wavelength  $\lambda \approx 0.89\mu\text{m}$ . The mass and the luminosity of  $\beta$  Pic are about  $2M_\odot$  and  $10L_\odot$ , respectively. These dust clouds are far outside the planet-forming regions obtained in Section 3. We shall investigate the origin and the present status of these clouds.

##### 4.1. Regions of Planetesimal Formation

Because planetesimals form by sedimentation of dust in the gaseous nebula, the outer boundary of the planetesimal-forming region depends on the time when the gaseous nebula is blown away. If the gaseous nebula around a star of  $M_* = 2M_\odot$  survives up to the end of the Hayashi phase  $t_{\text{EHP}} \approx 2 \times 10^6 \text{yr}$ , the outer boundary is around 530AU as long as the gaseous nebula extends at least out to this radius. Similarly for  $M_* = 3M_\odot$  with  $t_{\text{EHP}} \approx 5 \times 10^5 \text{yr}$ , the outer boundary is around 250AU. If the gaseous nebula is blown away before the dust sinks, the solid material is also blown away together with the gas.

4.2. Random Motion of Planetesimals

Because the gaseous nebula is blown away in the early stage of the stellar evolution, the planetesimals in the outer region spend most of their life in the gas-free state. Therefore, the time variation of their random velocity  $v$  is described by equation (14) with  $t = \infty$ . Because  $v$  is initially very small and the available time is too short to attain the equilibrium given by equation (17),  $t_E$  is much smaller than  $t_C$ . In addition, because  $t_C$  is much greater than the stellar lifetime, the mass of the planetesimal is nearly equal to the initial value  $m_0$ . Then, equation (14) is easily integrated as

$$i \approx v/v_K = (13 \pi^2 \ln \Lambda)^{1/4} M_*^{-1/2} (m_0 r^2 \sigma_s t / t_k)^{1/4} \\ \propto \zeta f_\sigma M_*^{-1/24} r^{1/8} t^{1/4} . \tag{23}$$

The last expression in equation (23) is for  $\sigma$  given by equation (1).

Figure 3 shows the mean inclination of planetesimal's orbit for  $M_* = 2M_\odot$  and  $f_\sigma = 3$  at some epochs. Each line is labeled with the value of  $t$  in units of  $10^8$  yr. The straight lines in the outer region come from equation (23). In the inner region the random velocity is nearly in a steady state and the growth of planetesimals is taken into account. The inner end of the curve is at the outer edge of the region where planets have already formed at each epoch. At  $t = 1 \times 10^8$  yr the mean inclination at  $r = 300$  AU is about  $3^\circ$  and is consistent with the thickness of the  $\beta$  Pic disk.

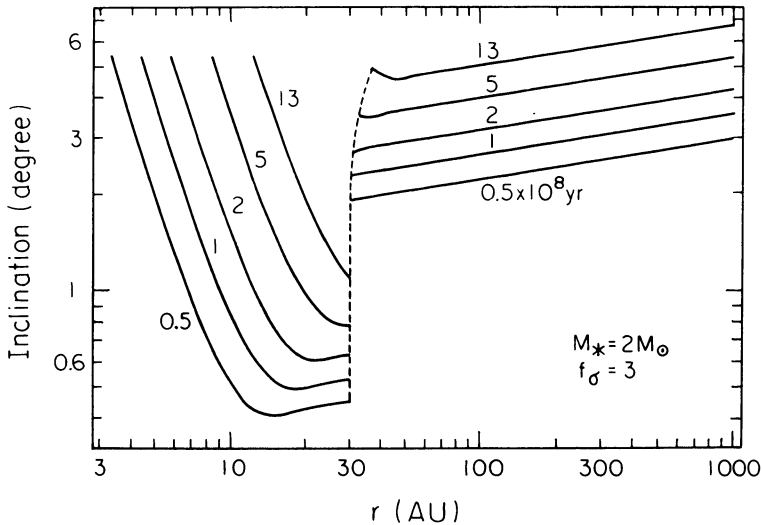


Fig.3. The mean orbital inclination of planetesimals as a function of the distance  $r$  from the star at some stages for  $M_* = 2M_\odot$  and  $f_\sigma = 3$ . Each line is labeled with the value of  $t$  in units of  $10^8$  yr.

### 4.3. Collisions of Planetesimals

From equations (5), (7), (8) and (23) the number of collisions that each planetesimal has experienced up to  $t$  is given by

$$N_c(r, t) = \int_0^t t_c^{-1} dt = (3.17M_*/\rho_s r^3)^{2/3} t/t_K + 2.22(\ln \Lambda)^{-1/2} (3.17M_*/\rho_s r^3)^{1/3} (t/t_K)^{1/2}. \quad (24)$$

Even at the end of the stellar life  $t = 1.3 \times 10^9$  yr for  $M_* = 2M_\odot$ , we have  $N_c = 0.19$  and  $0.048$  at  $r = 100$  and  $200$  AU, respectively. Thus only a small fraction of the planetesimals undergo collisions in the outer region. When  $N_c \ll 1$ , the second term in equation (24) is dominant. Although the collision is mostly coalescent, some small particles are scattered. Because small particles are numerous, they collide with each other frequently. Collisions of small particles with negligible gravity must be mostly destructive. The circumstellar dust cloud is inferred to form by the collisions of such small particles.

### 4.4. The Surface Brightness of the Dust Disk

The radiation of the central star is scattered mainly by the small particles. The intensity  $F \Delta\Omega$  of the scattered light from the dust along the light of sight into a solid angle  $\Delta\Omega$  is given by

$$F \Delta\Omega = \frac{\Delta\Omega}{4\pi} A \epsilon \int \sigma_s(r') (2i(r')r')^{-1} N_c(r', t) f_s(r', t) L_*(t) (4\pi r'^2)^{-1} dx, \quad (25)$$

where  $A$  is the albedo of the dust,  $\epsilon$  is the mass fraction of solid matter which becomes small particles due to collisions,  $r'$  is the distance from the star,  $f_s$  is the ratio of the cross section to mass of small particles,  $L_*$  is the stellar luminosity, and the integration is along the line of sight. We assume that the small particles have a size distribution  $n(a)da \propto a^{-3.5} da$ , where  $a$  is the radius. The size distribution of the asteroids can be approximated by this law (Hughes 1982; Ishida et al. 1984). Both analytic and numerical investigations show that the size distribution of solid bodies under collisional fragmentation is also well represented by this law (Dohnanyi 1969; Hellyer 1970, 1971). For this size spectrum we have

$$f_s = (3/4\rho_s) (a_1 a_2)^{-1/2}, \quad (26)$$

where  $a_1$  and  $a_2$  are, respectively, the minimum and maximum radii. The minimum size is determined by the Poynting-Robertson effect as (Allen 1973)

$$a_1 = 3L_* t / (4\pi c^2 \rho_s r^2), \quad (27)$$

where  $c$  is the light speed.

From these considerations the surface brightness of (energy flux from) the part of the edge-on disk, subtending a solid angle  $\Delta\Omega$  to the observer, is given by

$$F_{\text{edge}}(r,t)\Delta\Omega = 1.75 \times 10^{-3} \Delta\Omega A \epsilon cG^{1/8} \rho_s^{-5/6} (\ln \Lambda)^{-3/4} (L_*/a_2)^{1/2} M_*^{35/24} t^{-1/4} r^{-35/8}. \quad (28)$$

It is to be noticed that  $F_{\text{edge}}$  is independent of  $\sigma_s$ . It decreases slowly with time as  $t^{-1/4}$ . The  $r$  exponent,  $35/8 = 4.375$ , is very close to 4.3, the exponent obtained from the observations of the  $\beta$  Pic disk. The surface brightness of the  $\beta$  Pic disk at  $r = 100\text{AU}$  is  $16 \text{ mag/arcsec}^2$  at  $\lambda = 0.89\mu\text{m}$  (Smith and Terrile 1984). This brightness is obtained from equation (28) with the reasonable values of the parameters  $M_* = 1.8M_\odot$ ,  $L_* = 10L_\odot$ ,  $t = 10 \text{ yr}$ ,  $A = 0.2$ ,  $\epsilon = 0.1$ , and  $a_2 = 50\text{cm}$ .

The surface brightness of the disk seen face-on is given by

$$F_{\text{face}}(r,t)\Delta\Omega = 1.27 \times 10^{-2} \Delta\Omega A \epsilon cG^{1/4} \rho_s^{-5/6} (L_*/a_2 \ln \Lambda)^{1/2} M_*^{7/12} \sigma_s r^{-11/4}. \quad (29)$$

For  $\sigma$  given by equation (1),  $F_{\text{face}}$  is proportional to  $f_\sigma M_*^{17/12} r^{-17/4}$ . The  $r$  exponent,  $17/4 = 4.25$ , is very close to that for the edge-on disk. This surface brightness changes with time only through  $L_*$ .

#### 4.5. The Optical Thickness of the $\beta$ Pic Disk

Beta Pictoris with a spectral type of A5V is fainter than an unobscured A5V star by 0.3 to 0.8 magnitudes. Because no reddening has been found in the spectrum of  $\beta$  Pic, most of the obscuration must come from the circumstellar dust cloud. Therefore, the optical thickness of the dust cloud between the star and us is between 0.3 and 0.7.

If the above model disk with  $f_\sigma = 3$  which explains well the thickness and the surface brightness of the  $\beta$  Pic disk is seen strictly edge-on, the optical thickness of the parts  $r = 4$  to  $11\text{AU}$ ,  $11$  to  $16\text{AU}$ ,  $16$  to  $25\text{AU}$ , and  $r > 25\text{AU}$  is 0.42, 0.32, 0.14, and 0.12, respectively. Therefore, the total optical thickness is about 1.0. However, if the disk has an inclination of  $1^\circ$  to us, the region between 9 and  $25\text{AU}$ , where the mean inclination of the orbit is less than  $1^\circ$  as seen in Figure 3, does not contribute to the optical thickness. Therefore, the total optical thickness is about 0.4, consistent with the observations.

Thus, the geometrical and optical thickness and the surface brightness distribution of the  $\beta$  Pic disk are explained with our model which has been constructed with some simple reasonable assumptions.

#### REFERENCES

- Allen, C.W., 1973. *Astrophysical Quantities* (Athlone Press, London), p.157.

- Aumann, H.H., Gillett, F.C., Beichman, C.A., de Jong, T., Houck, J.R., Low, F.J., Neugebauer, G., Walker, R.G., and Wesselius, P.R., 1984. *Astrophys. J.*, 278, L23.
- Cameron, A.G.W., and Pine, M.R., 1973. *Icarus*, 18, 377.
- Chandrasekhar, S., 1942. *Principles of Stellar Dynamics* (University of Chicago Press, Chicago; Dover Publications, Inc., New York), p.48.
- Cox, L.P., and Lewis, J.S., 1980. *Icarus*, 44, 706.
- Dohnanyi, J.S., 1969. *J. Geophys. Res.*, 74, 2531.
- Fujiwara, A., and Tsukamoto, A., 1980. *Icarus*, 44, 142.
- Gaustad, J.E., 1963. *Astrophys. J.*, 138, 1050.
- Goldreich, P., and Lynden-Bell, D., 1965a. *Mon. Not. Roy. Astron. Soc.*, 130, 97.
- Goldreich, P., and Lynden-Bell, D., 1965b. *Mon. Not. Roy. Astron. Soc.*, 130, 125.
- Greenberg, R., Wacker, J.F., Hartmann, W.K., and Chapman, C.R., 1978. *Icarus*, 35, 1.
- Greenberg, R., Weidenschilling, S.J., Chapman, C.R., and Davis, D.R., 1984. *Icarus*, 59, 87.
- Grossman, L., 1972. *Geochim. Cosmochim. Acta*, 36, 597.
- Hartmann, W.K., 1978. *Icarus*, 33, 50.
- Hayashi, C., 1981. *Prog. Theor. Phys. Suppl.*, No. 70, 35.
- Hayashi, C., Nakazawa, K., and Adachi, I., 1977. *Publ. Astron. Soc. Japan*, 29, 163.
- Hayashi, C., Nakazawa, K., and Nakagawa, Y., 1985. *Protostars and Planets II*, ed. D.C. Black and M.S. Mathews (University of Arizona Press), p.1100.
- Hellyer, B., 1970. *Mon. Not. Roy. Astron. Soc.*, 148, 383.
- Hellyer, B., 1971. *Mon. Not. Roy. Astron. Soc.*, 154, 279.
- Hubbard, W.B., MacFarlane, J.J., Anderson, J.D., Null, G.W., and Biller, E.D., 1980. *J. Geophys. Res.*, 85, 5909.
- Hughes, D.W., 1982. *Mon. Not. Roy. Astron. Soc.*, 199, 1149.
- Ishida, K., Mikami, T., and Kosai, H., 1984. *Publ. Astron. Soc. Japan*, 36, 357.
- Matsui, T., and Mizutani, H., 1977. *Nature*, 270, 506.
- Matsui, T., and Mizutani, H., 1978. *Icarus*, 34, 146.
- Nakagawa, Y., Hayashi, C., and Nakazawa, K., 1983. *Icarus*, 54, 361.
- Nakagawa, Y., Nakazawa, K., and Hayashi, C., 1981. *Icarus*, 45, 517.
- Nakano, T., 1986. in preparation.
- Safronov, V.S., 1969. *Evolution of the Protoplanetary Cloud and Formation of the Earth and the Planets* (Israel Program for Scientific Translations).
- Sekiya, M., 1983. *Prog. Theor. Phys.*, 69, 1116.
- Sekiya, M., Nakazawa, K., and Hayashi, C., 1980. *Prog. Theor. Phys.*, 64, 1968.
- Smith, B.A., and Terrile, R.J., 1984. *Science*, 226, 1421.
- Takeda, H., Matsuda, T., Sawada, K., and Hayashi, C., 1985. *Prog. Theor. Phys.*, 74, 272.
- Toomre, A., 1964. *Astrophys. J.*, 139, 1217.

TERRILE: In regard to the optical thickness of the Beta Pictoris disk, the inner region of the disk will not contribute to the total optical depth because material will have been cleared out by planet formation

NAKANO: You are right. With my model at  $t = 1 \times 10^8$  yr, for example, planets have already formed inside about 4 AU.

NORMAN: In your scheme, when do the planets form? In the molecular disk era, the T-Tauri-phase, or later. What can observers look for, for example, in the early stages of planetary formation even in molecular disk e.g. sedimented dust disks - CO disks?

NAKANO: For  $M_* = 1 M_\odot$  with  $f\sigma = 2$ , for example, a planet forms at  $t = 2 \times 10^6$  yr at  $r = 1$  AU and at later stages in the outer region. Because the era of bipolar flow would continue for less than about  $10^5$  yr, the planets form in the T-Tauri and later phases. Because the gaseous nebula has a very high surface density, it is opaque to most of the molecular lines. In addition, the planet-forming region has a very small surface area. Therefore the intensities of any molecular lines from the disk are very weak.